One-million year Rare Earth Element stratigraphies along an Antarctic marine sediment core

Francesco Rugi[a]

Roberto Udisti[a]

Silvia Becagli[a]

Daniele Frosini[a]

Giovanna Giorgetti[b]

Gerhard Kuhn[c]

Miriam Marconi[a]

Donata Monien[d]

Silvia Nava[e]

Mirko Severi[a]

Franco Talarico[b]

Rita Traversi[a, *]

rita.traversi@unifi.it

[a]Department of Chemistry "Ugo Schiff", University of Florence, Via della Lastruccia, 3, I-50019 Sesto Fiorentino (FI), Italy

[b]Department of Earth Sciences, University of Siena, Via Laterina 8, Siena, Italy

[c]Alfred Wegener Institute for Polar and Marine Research, Am Alten Hafen 26, Bremerhaven, Germany

[d]Institute for Chemistry and Biology of the Marine Environment, Carl-von-Ossietzky University Oldenburg, Carl-von-Ossietzky Straße 9-11, 26129 Oldenburg, Germany

[e]Department of Physics and Astronomy, University of Florence and National Institute of Nuclear Physics (INFN), Via G. Sansone 1, 50019 Sesto Fiorentino (Fi), Italy

*Corresponding author. Tel.: + 39 0554573381, + 39 3478747270 (mobile).

Abstract

An integrated system, based on Inductively Coupled Plasma—Sector Field Mass Spectrometry (ICP-SFMS) and Inductively Coupled Plasma—Atomic Emission Spectrophotometry (ICP-AES) techniques, was optimised for the geochemical characterisation of soils and marine sediments. Sample mineralization was carried out with HF, HNO_3 and $HClO_4$. Operative blanks were at least two orders of magnitude lower than the lowest concentration measured in real samples. For ICP-SFMS, the detection power of the method in high resolution mode was sufficient for an accurate quantification of metals, yet avoiding REEs (Rare Earth Elements) isobaric interferences. Once tested the accuracy on six certified materials, the methods were applied to the analysis of 39 major and trace metals on the top 90 m of sediments from the ANDRILL AND-1B core, covering the last million years.

Stratigraphies of REEs and of normalised markers from this core clearly highlight a discontinuity at about 660,000 years before present. This pattern is well shown by the results of a PMF (Positive Matrix Factorization) statistical analysis, revealing two different sources for the sedimentary material, whose relative contribution changed around that time. Such a result is consistent with previous studies and confirms the net change in the provenance of glacial fluxes in the McMurdo region (Ross Ice Shelf, Antarctica) in the last million years.

1 Introduction

REEs have been widely used as excellent proxies for several geochemical processes in cosmogenic chemistry, igneous petrology, and sedimentology. Indeed, REEs are fractionated in the environment because the progressive increase of the charge/radius ratio with the atomic number (the so-called lanthanide contraction) causes small but systematic differences in their chemical properties. Besides, due to their low solubility and scarce mobility in the terrestrial crust, REEs display a conservative behaviour in the environment [7]. As a consequence, REEs abundance varies in weathering products, and their relative changes are used as a marker of source rocks [16,31].

The Antarctic cryosphere (the complex system composed by the continental ice cap, coastal ice shelves, sea-ice, and marine sediments) is considered one of the most precious archives of paleo-enviromental and paleo-climatic information (EPICA—European Project for Ice Coring in Antarctica [5]; EPICA [6,23]). Indeed, the surface and volume changes of the Antarctic ice cap, as a consequence of climate forcings, play a critical role in the climatic system and constitute complex feedbacks with hydrosphere, atmosphere, lithosphere, and biosphere. In particular, changes in ice-volume affect the global sea level, Earth albedo, atmospheric and oceanic circulation, marine productivity, and greenhouse gas emissions and uptake processes. Such environmental changes, in turn, affect the solar irradiance budget and the global transport and distribution of matter and energy [1,12].

In this context, one of the main goals of the ANtarctic DRILLing Program (ANDRILL) was to gather information on past changes in the Antarctic climate and on the dynamics of the Antarctic ice cap over the last 35 millions of years (Ma), by a geochemical, mineralogical, and palaeontological characterisation of two deep sediment cores drilled in the Ross Sea region, which is close to the current margin of the Ross Sea Ice Shelf [9]. In particular, detailed palaeo-climatic and palaeo-enviromental information can be obtained from sedimentological, geochemical, and geophysical stratigraphies of the ANDRILL-MIS (McMurdo Ice Shelf) B1 sediment core (AND-B1, 1260 m deep, covering the Plio—Pleistocene period: 0–15 Ma ago), composed by glaciomarine, terrigenous, volcanic, and biogenic sediment that has accumulated in the Windless Bight region of a flexural moat basin surrounding Ross Island.

In this paper, we report the first results on the geochemical stratigraphy of the uppermost 90 m of the AND-B1 core, roughly covering the last one million years, by an analytical set-up developed for the sample mineralisation and the determination of 39 major and trace elements, including REEs.

The element quantification was carried out by an integrated system with Inductively Coupled Plasma (ICP) Atomic and Emission Spectrophotometry (ICP-AES) or High-Resolution Sector-Field Mass Spectrometry (ICP-SFMS) detectors, depending on element concentrations and interferences.

A multi-element internal standard method was used to correct matrix effects. An accurate quantification of the residuals after internal standard correction allowed identifying signal temporal drifts which are different element by element. The correction of such drifts, by periodical repetitions of a multi-standard and of a certified material solution, significantly improved reproducibility and accuracy. The improved detection limits for all the REEs allowed using the high resolution technique $(10,000 \ m/\Delta m)$ in their determination by ICP-MS, hence avoiding possible isobaric interferences.

Single-metal recovery and accuracy were evaluated by using a set of marine sediments (NIST 2702, GBW 07313, CRM-MURST-ISS-A1) and soil (Basalt, Hawaiian Volcanic Observatory BHVO-1, Japanese andesite JA-2, Montana soil NIST 2711) certified materials; the results are reported in Tables 1 and 2 in the Supplementary material.

2 Materials and methods

Sample mineralisation was carried out with a mixture of ultrapure HNO_3 (69.5% reagent grade, purified by sub-boiling distillation — s-b d.), HF 40% (Suprapur grade), and $HClO_4$ 70% (Suprapur grade).

Three internal standards were used for ICP-SFMS analyses (In, Re and Ge at 12, 30, and 60 $\mu g \ L^{-1}$, respectively) and a mono-element internal standard (Ge, 5 $mg \ L^{-1}$) was used for ICP-AES analyses.

Detailed information about reagents and standard solutions are reported in the Supplementary material.

2.1 Instrumentation

Analytical measurements were carried out using a Sector-Field ICP mass spectrometer and an ICP-AES spectrophotometer. The instrumental set-up conditions are reported in Table 3 in the Supplementary material.

Analytical performances obtained in this paper allowed performing ICP-MS measurements in the high resolution mode for analysing trace metals and REEs in all the AND-B1 samples. In this way, isobaric interferences were minimised. The main interferences occurring in low- and high- resolution (LR: 1000 $m/\Delta m$; HR: 10,000 $m/\Delta m$) modes are listed in Table 4 in the Supplementary material. Although a few elements or molecular species interfere on the determination of some analytes also in the HR mode, they are present in soils and marine sediments at very low concentrations and their contribution to the analytical signal is negligible (at least, two orders of magnitude lower than the background levels).

2.2 Method set-up

2.2.1 Sample mineralisation

A mineralization procedure with HNO_3 + HF + $HClO_4$, slightly modified with respect to the methods reported in literature [3,19,20,27,29,33,34] was used. The formation of poorly soluble fluorides, especially with Zr, Hf, and REEs, was minimised by removing HF after mineralization [33]. Samples were freeze-dried, coarsely (2 mm) sieved and milled up to size homogenization by an agate ball mill. An aliquot of about 100 mg (accurately weighed) was placed into a pre-washed 15-mL PFA Savillex vial and 2 mL of s-b d. HNO_3, 3 mL of s.p. HF and 3 mL of s.p. $HClO_4$ were added. The sealed vials were mineralised following the procedure in detail reported in the Supplementary material. Mineralised solutions were stored at + 4 °C and analysed within 48 hoursh after dissolution.

Although micro-wave digesters were available, the hot-plate technique was chosen in order to standardize the mineralization procedure inside the ANDRILL geochemistry consortium. Mineralization recovery, accuracy and reproducibility were successfully tested on certificated materials.

2.2.2 Reproducibility, detection limits and reagent blank

Reproducibility (RSD), Limits of Quantification (L.O.Q.) and blank values are shown in Table 1. Single-element reproducibility was evaluated by 10 repetitions of multi-element standard solutions. The ICP-MS (HR mode) RSD was better than 3% at 1 µg/L level. For ICP-AES, RSD was better than 1.5% at 10 µg/L level, with few exceptions: Fe (2.3%), K (4.3%) and Ca (8.8%). The relatively poor RSD for Ca is due to the high blank contribution, but it does not affect the real sample measurements, where Ca concentrations are as high as 1 mg/L (see below).

Table 1 Basic analytical performances of ICP-SFMS and ICP-AES techniques. ICP-SFMS: analytical masses, detection limits, blank levels, RSD%, and internal standards applied. ICP-AES: Wavelengths, detection limits, blank levels, RSD%, and internal standards applied.

		ICP-SFMS Finnigan MAT Element2			
Element	Analytical mass	D.L. (ng L^{-1})	Blank (ng L^{-1})	RSD % (1 µg L^{-1})	Internal standard
Ce	^{140}Ce	8.4	d.l.	0.8	^{115}In
Cr	^{52}Cr	9.1	127.9	1.1	^{115}In
Cs	^{133}Cs	3.6	d.l.	1.1	^{115}In
Dy	^{163}Dy	10	d.l.	2.0	^{185}Re
Er	^{166}Er	9.9	d.l.	2.2	^{185}Re
Eu	^{151}Eu	11.2	d.l.	1.7	^{115}In
Gd	^{157}Gd	15.6	d.l.	1.6	^{115}In
Hf	^{178}Hf	13.8	38	2.3	^{185}Re
Ho	^{65}Ho	7	d.l.	1.1	^{185}Re
La	^{139}La	10.4	d.l.	1.3	^{115}In
Lu	^{175}Lu	5.4	d.l.	1.5	^{185}Re
Nb	^{93}Nb	6.7	27.8	0.8	^{72}Ge
Nd	^{146}Nd	13.9	d.l.	2.7	^{115}In
Ni	^{60}Ni	15	133.6	2.5	^{72}Ge
Pr	^{141}Pr	5.9	d.l.	0.8	^{115}In
Rb	^{85}Rb	12	20.9	1.3	^{72}Ge

Sc	^{45}Sc	9	11.3	1.3	^{72}Ge
Sm	^{147}Sm	14.2	d.l.	2.0	^{115}In
Ta	^{181}Ta	6.4	38	1.4	^{185}Re
Tb	^{159}Tb	5.8	d.l.	1.4	^{185}Re
Th	^{232}Th	11	d.l.	1.3	^{185}Re
Tm	^{169}Tm	6.9	d.l.	1.3	^{185}Re
U	^{238}U	4	d.l.	1.3	^{185}Re
Y	^{89}Y	7	d.l.	1.2	^{72}Ge
Yb	^{172}Yb	8.9	d.l.	1.4	^{185}Re
Zr	^{90}Zr	18.9	254.1	1.6	^{72}Ge

ICP-AES Varian 720-ES

Element	Wavelength (nm)	D.L. (μg L^{-1})	Blank (μg L^{-1})	RSD % (10 μg L^{-1})	Internal standard (nm)
Al	396.152	0.46	1.8	0.8	Ge 209.426
Ba	455.403	0.023	0.11	0.1	Ge 209.426
Be	313.107	0.016	0.019	0.1	Ge 209.426
Ca	317.933	0.68	7.1	8.8	Ge 209.426
Co	230.786	0.28	0.38	0.6	Ge 209.426
Fe	238.204	0.14	1.3	2.3	Ge 209.426
K	766.491	0.51	1.8	4.3	Ge 209.426
Li	670.783	0.034	0.39	0.3	Ge 209.426
Mg	285.213	0.13	0.9	0.6	Ge 209.426
Mn	257.61	0.029	0.1	0.2	Ge 209.426
Na	588.995	0.25	2.1	1.5	Ge 209.426
Sr	407.771	0.019	0.089	0.2	Ge 209.426
Ti	336.122	0.079	0.28	0.4	Ge 209.426

L.O.Q. values were calculated as 10σ of 10 repetitions of one standard solution containing 40 ng L^{-1} (ICP-SFMS) or 2 μg L^{-1} (ICP-AES) of each element.

ICP-SFMS and ICP-AES L.O.Q. values ranged from 12 to 63 ng L^{-1} and from 0.05 to 2.27 μg L^{-1}, respectively. We have to notice that such low ICP-SFMS detection limits were obtained operating in the HR mode, where sensitivities are significantly lower than those gained by LR techniques (e.g., ICP-QMS) but working in the HR mode allowed minimising the isobaric interferences.

Reagent blank values were at least two orders of magnitude lower than their minimum concentrations measured in the samples and in the certified materials (Table 1).

2.2.3 Real-sample improved quantification procedure

ICP-MS measurements are affected by significant signal fluctuation or noise and several internal-standard methods have been proposed to correct matrix effects on the quantification of elements in soils and sediments [4,11,28]. However, such methods

do not account for the residual noise after internal-standard correction.

Here, we discussed and quantified the residual noise and applied a successful correction by using a suitable internal standard procedure.

The quantification procedure was carried out by a 6-point external standard calibration curve, corrected by multiple internal standard additions (60 µg L^{-1} ^{172}Ge + 12 µg L^{-1} ^{115}In + 30 µg L^{-1} ^{185}Re spikes). The three internal standards cover light, medium, and heavy isotopic mass ranges, but the most suitable internal standard was chosen as a function of the single element (see last column in Table 1).

The internal-standard procedure allows correcting for the matrix effects that occur in the nebulisation and ionisation plasma processes and during the ion path from the extraction lens to the detector. As a consequence, the signal decreases over time with different trends for the different isotopes, with deeper drops for low-mass elements when large concentrations of heavy metals are present in the sample [24]. This mass-selective pattern was related to the poor transmission of ions through the ion optics due to matrix-induced space-charge effects [30].

To evaluate this effect, a multi-standard solution was measured at the beginning of the analysis session and after 5, 10, and 15 measurements of marine-sediment samples. Since each analysis lasts 12 min (including washing and 16 mass scans to increase by a factor 4 the signal/noise ratio), every sequence (5 samples and one standard solution) takes 1.2 hours. The trend of the normalised sensitivity is shown in Fig. 1a. As expected, the drop is mass-sensitive: the highest variations (~ 40% after 3.6 h) occur in the mass region < 100 amu. Fig. 1a clearly shows that the decreasing trend is different for each element and a number of internal standards as large as possible is usually used to correct the signal [4] thus increasing the method complexity.
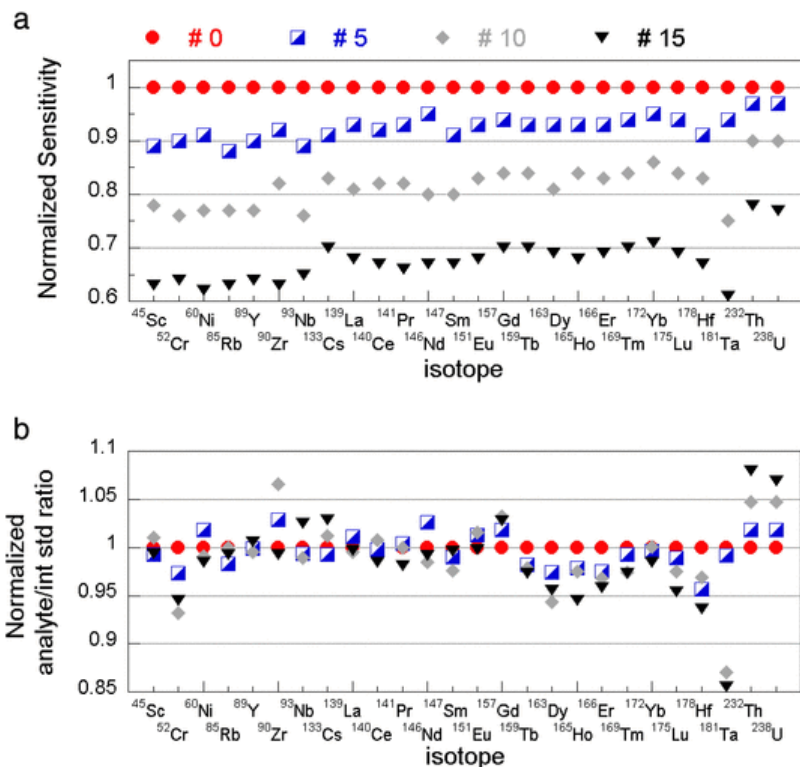

Fig. 1 Analytical sensitivity for each measured element isotope (a) Normalized sensitivity changes for all isotopes utilised in our analytical method during the course of an analytical run (about 1.2 hours); # indicates the number of real samples analysed from the start of the analytical run to the acquisition of the signals of the standard solution. (b) Normalised analyte/internal standard signal ratio (normalised with respect to the values obtained in run # 0) of each isotope as a function of atomic mass unit; # indicates the number of real samples analysed from the start of the analytical run to the acquisition of the signals of the standard solution.

We used a different approach. Using just 3 internal standards strongly reduces temporal drifts but, as expected, does not eliminate them. Fig. 1b shows the residual drifts (after 5, 10, and 15 samples) for each isotope, after the internal-standard correction. The residual drifts appear to be composed of two components: a random component associated to the reproducibility (relative standard deviation, RSD, usually lower than 2%) and a progressive bias component that depends on changes of the room and spray

chamber temperatures, detector response, and cone occlusion.

As the drift is usually lower than 5% after a 5-sample sequence, we applied a single-isotope correction, assuming a linear trend of the signal variation between two consecutive repetitions (spaced by 5 samples) of the multi-standard solution. Besides, in order to monitor the accuracy, the central sample (sample 3 of each 5-samples group) was periodically replaced with a certified-material sample.

For ICP-AES measurements, no temporal drift by matrix effects was observed and a single internal-standard method was used (5 mg/L Ge).

2.2.4 Real-sample methods performances

The real-sample RSD was evaluated by 10 repetitions of a mineralised sample. ICP-MS RSD, was always lower than 6.5% and better than 3% for the majority of the elements (Fig. 1a Supplementary material). For ICP-AES, the RSD was lower than 1.5 % for all the metals (Fig. 1b Supplementary material).

The overall accuracy, including mineralisation, was tested by analysing six certified reference materials (3 soils and 3 marine sediments): BHVO-1, JA-2, NIST 2711, GBW 07313, NIST 2702, and CRM-MURST-ISS-A1. The results are shown in Tables 1 (marine sediments) and 2 (soils), in Supplementary material. Concentrations were calculated as the mean value of the analysis of different aliquots of the same certified material (from 3 to 8 mineralizations were carried out for each certified material). The RSD were typically lower than 10% for ICP-SFMS and lower than 5% for ICP-AES.

Relative percentage errors (RPE) are shown in Fig. 2a and b (Supplementary material). RPE are usually lower than 15% (lower than 10% for most of the elements). Higher errors were obtained for elements labelled as "Recommended Values", such as Cs and Sc in GBW 07313, La in NIST 2702, and Ba and Be in BHVO-1. When compared to "Indicated values", differences are still larger, especially for Th, U, Zr, and Hf. Part of this difference can be ascribed to the lower efficiency of the acidic mineralization of refractory minerals (such as zircon, sphene, spinel, and garnet) in which Th, U, Zr, and Hf are included [27]. A more efficient extraction of these metals from soils and sediments could be carried out using a sodium peroxide sinter or lithium borate fusion. However, sinter or fusion methods can be affected by contamination from large reagent quantities and possible loss of volatile elements [27].

Literature results show ICP-MS RSD in the range 3–10% and accuracy errors lower than 10% [2,10,14,19,21,25,26,28,32]. For some heavy REEs (HREEs), a lower accuracy (10–25%) was obtained by Liang and Gregoire [19]. Such results were usually obtained by using a large number of internal standards: for instance, 9 internal standards made of 4 enriched and 5 natural isotopes [4]. On the contrary, our method allows obtaining comparable results just using three internal standards, thus lowering costs (enriched isotopes are expensive) and simplifying the quantification procedure.

3 Results and discussion

The methods were applied in quantifying major and trace elements in the first 90 m of the AND-1B sediment core. ANDRILL is an international project aiming to understand the response of the Ross Ice Sheet to the climate forcings during the Pleistocene (1.8 Ma) [9]. In this framework, AND-1B core was drilled in the 2007 up to the depth of about 1650 m, probably covering the last 15 Ma of Earth climatic history. The uppermost part of the AND-1B core was Ar/Ar dated and the first 90 m recorded the sedimentation processes occurred in the last 1.0 Ma [23], a time interval similar to that covered by the EPICA Dome C ice core, drilled in East Antarctica, i.e. about 900 kyr (EPICA [6]).

Here, we present the first detailed REEs stratigraphy in the 24.7–89.0 m depth range, covering roughly the time period 400–1050 kyr. Analysis was carried out on sub-samples 2 to 3 cm thick at 1-metre intervals. The first 25 m were as not analysed because the sedimentary sequence was perturbed by the drilling operations. Besides, massive volcanic layers, identified by high resolution X-Ray Fluorescence–Core Scanner analysis (XRF-CS) [13], were removed due to their poor significance in pointing out different patterns in sediment-source contributions from changes in continental glacial fluxes.

Fig. 2 shows the depth profiles of the REEs measured in the sediment samples (La, Ce, Pr, Nd, Sm, Eu, Gd, Tb, Dy, Ho, Er, Tm, Yb, Lu).
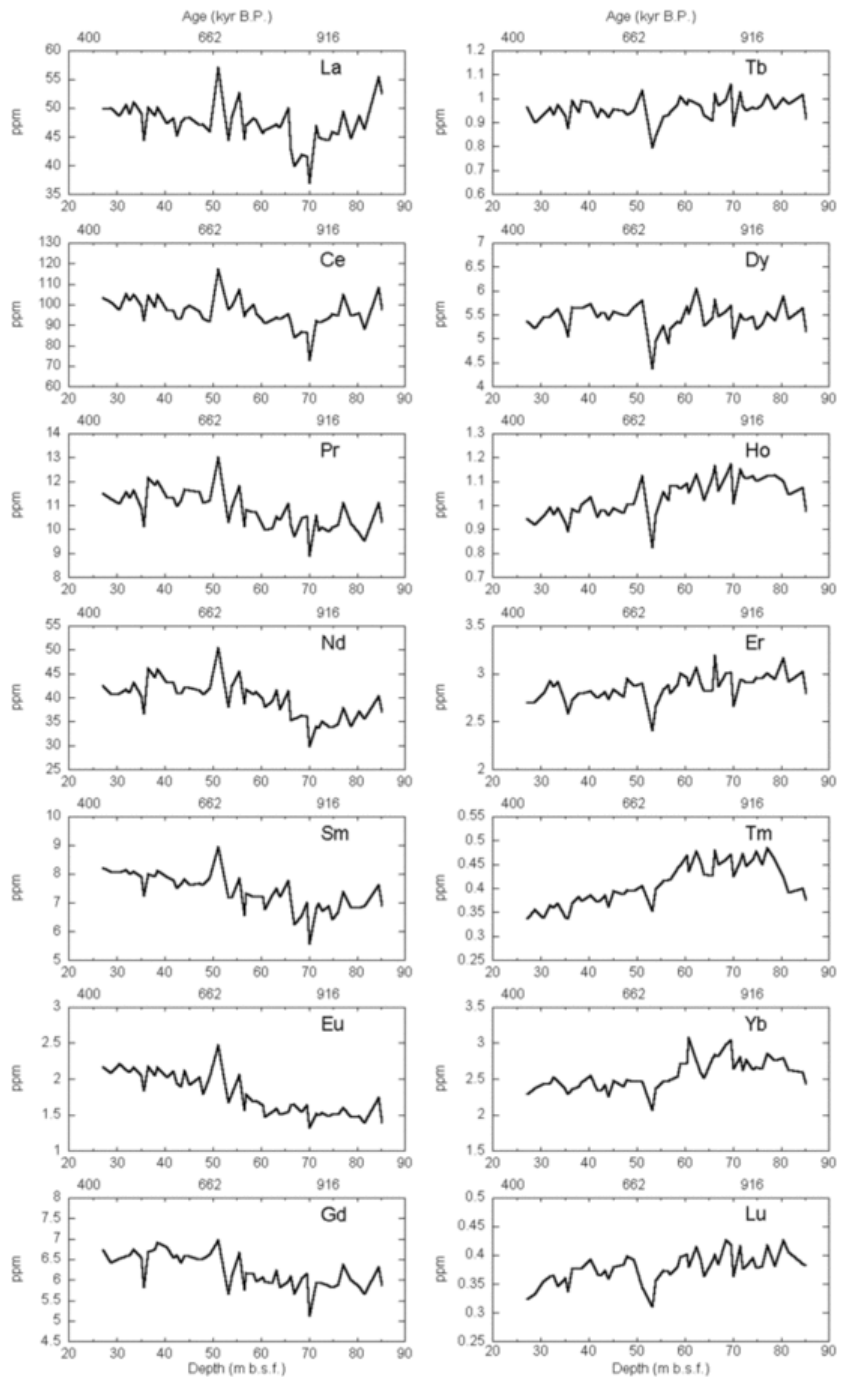
elsevier_MICROC_2131

Fig. 2 Stratigraphy of Rare Earth Elements along the analysed core.

Concentration vs. depth trends of all the REEs determined along the AND-1B core. The bottom x-scale represents depth while the up x-scale indicates age (as kyr Before Present).

From a general point of view, one can observe a large variability in concentration of all the REEs along the whole analysed core. Despite such an intrinsic variability, a feature can be detected. In the depth range 70–50 m, roughly corresponding to the time interval 860–660 kyr BP, REEs elements show a progressive trend as function of their atomic number. From La to Gd, we can observe a clear concentration increase as the depth decreases. On the contrary, from Tb to Lu the concentration decrease as the depth decreases. Conventionally, REEs elements are split in light REEs (LREEs), from La to Nd, and heavy REEs (HREEs), from Sm to Lu. However, this classification does not seem to be so constraining because the chemical properties of the REEs change in a very progressive way as the atomic number increases. In addition, the observed pattern does not seem to be consistent with such classification. For these reasons, the clear opposite pattern drives us to classify the REEs in differently arranged sub groups. In this sense, thereafter the label LREEs refers to the La–Gd elements, and the notation HREEs is attributed to the Tb–Lu group. It is reasonable to assume that the detected change in LREE and HREE concentrations could be the result of climatic forcing effects inducing differences in the glacial fluxes affecting the studied area. In order to better point out such discontinuity in the stratigraphic series, Fig. 3 shows some selected parameters as a function of depth: the LREE/HREE ratio, the so-called "Europium anomaly", and the Fe/Al ratio, as a marker of the crustal source. LREE and HREE values were calculated by summing the normalised values of every element belonging to the related REE group in all the depth range. The Eu anomaly is the phenomenon whereby the Eu concentration in a mineral is either enriched or depleted relative to the contiguous REEs (Sm and Gd). A positive (negative) Eu anomaly indicates that the mineral is Eu enriched (depleted) with respect to the chondrite, taken as a reference of the pristine crustal composition. The Fe/Al concentration ratio was calculated in order to: 1. remove the possible effect of differences in elemental concentrations due to the different grain-size distribution along the core; and 2. correct for possible dilution effects.
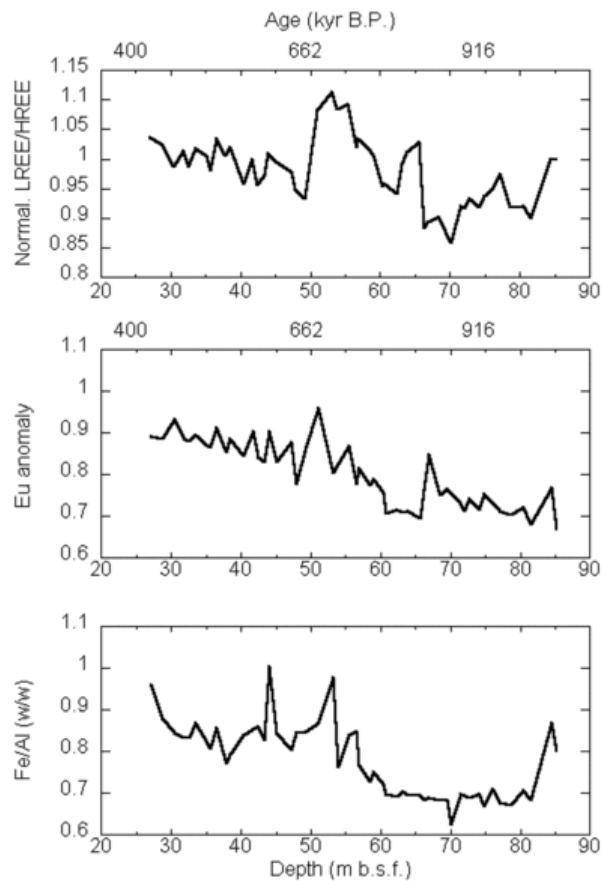

Fig. 3 Stratigraphy of relevant ratios and anomalies along the core.

Trends of Fe/Al, Eu anomaly and normalised LREE/HREE ratio as function of depth along the AND-1B core.

As already observed for the trends of single REEs, all the three parameters show two singular points around 70 and 50 m depth. For sediments deeper than 70 m, all the parameters show almost constant levels; for sections shallower

than 50 m, all parameters show a moderate increase; in the 70–50 m depth interval, a very sharp increase is shown by the three parameters; such increase is followed by a rapid drop, before the values continue to increase for depth lower than 50 m. This pattern is particularly evident in the LREE/HREE ratio. Indeed, a mineralogical clast analysis [8], performed on the same core section, showed a discontinuity in mineralogical assembles around 60 m depth. Giorgetti et al. [8] identified two main sources for the terrigenous material: the McMurdo Volcanic Group (MVG), which is dominant during most of the time, and Transantarctic Mountains (TAM), which plays a more relevant role in cold periods, when it is active a significant glacial flux from such source area to the sediment site. The latter contribution was found to be generally lower along the whole core, but increased up to 50% in the 50–70 m depth interval.

3.1 PMF statistical analysis

In order to identify and quantify the main sources of sedimentary material in the AND-1B core and to enlighten changes in the time of the relative contributions, a Positive Matrix Factorisation (PMF) analysis (see Supplementary material) was applied to the dataset. PMF analysis identifies three main sources of the sediment core material. Fig. 4 shows the sources profiles of sources 1 (S1, plot 4a), 2 (S2, plot 4b) and 3 (S3, plot 4c). Source profiles are expressed as absolute contribution (red bars: μg of each chemical component per g of sediment – mg/L) and as explained variance (black dots). We have to note that the greater is the explained variance of one element, the higher is its importance as source marker, independently from its absolute contribution. On the other hand, the mass of every source is the sum of the absolute contributions of all the elements found in this source. As concerning the major components, S1 source profile shows relative contributions of Fe and Ti higher than S2. The TiO_2 and Fe_2O_3 mean percentages are 2.3% and 8.6%, respectively. Such percentages are congruous with sediments coming from McMurdo Volcanic group (MVG). Indeed, MVG volcanic rocks vary from basanite to phonolite, with a mineral assemblage consisting in feldspathoid, plagioclase and augite, together with olivine and minor iron–titanium oxides [17]. The composition of MVG rocks is characterised by relatively high TiO_2 values (mostly higher than 2.5%), and Fe_2O_3 ranging between 7 and 13% [18].
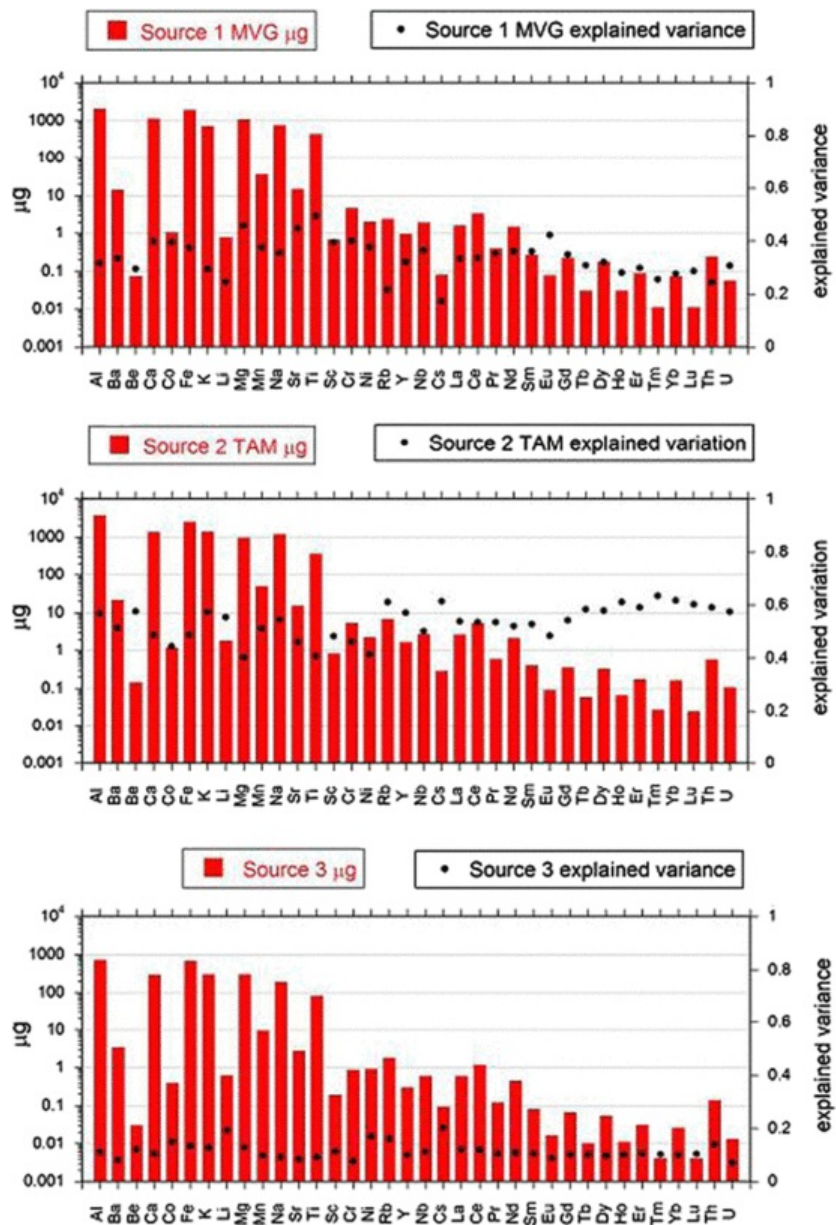
Fig. 4 Chemical profile of sediment sources as identified by using Positive Matrix Factorization.

Elemental profiles of the three sources (S1, S2, S3) identified by PMF analysis. Red columns refer to the mass (expressed as µg) of each element present in a source whereas blue dots refer to the explained variance of each metal in that source. (For interpretation of the references to colour in this figure legend, the reader is referred to the web version of this article.)

S2 source profile shows significantly lower percentages of TiO_2 (1.0%) and Fe_2O_3 (6.1%). This composition in major crustal elements could indicate sediments coming from the Trans Antarctic Mountain (TAM) source, especially from the Granite Harbour Intrusive Complex (GHIC), associated with metamorphic rocks and overlain by the Ferrar and Beacon supergroups. Detailed mineralogy and chemical composition of TAM rocks is reported in Monien et al. [22]. Their mean composition includes relatively low TiO_2

and Fe$_2$O$_3$ percentages (0.5–1% and 1–9%, respectively). Such values are consistent with the ones measured in the S2 source.

REEs contribute in S1 and S2 allow obtaining a more specific fingerprint of the two sources. S1 is characterised by high explained variances of LREE, (from La to Sm, other than Sc and Y), with respect to the HREE. Besides, S1 shows a high Eu explained variance, which is higher than that of the contiguous REEs, Sm and Gd.

On the contrary, HREE (from Gd to Lu) have higher explained variance than LREE in the S2 source profile. This evidence is a confirmation of the observed opposite trend of the LREE/HREE ratio before observed along the sediment core. Besides, S2 is characterised by two trace elements: Rb and Cs, that exhibit a higher explained variance with respect to S1. Finally, Eu presents a lower explained variance with respect to the contiguous Sm and Gd.

Unfortunately, the REEs cannot be used in identifying the original source because REEs data from MVG and TAM areas are missing. However, the hypothesized source attribution, made on the Fe$_2$O$_3$ and TiO relative contributions, can be confirmed by the temporal trend of the S1 and S2 sources (see below).

S3 identification is more difficult. Its profile (Fig. 4c) shows very low explained variance for almost all the components and does not seem to correspond to the source Southern TAM (S TAM) as reported in Monien et al. [22]. The contribution of this source to the sediment mass balance is generally lower than the other sources with the exception of few samples in sediment layers at 53.1, 56.6, 84.4 and 85.2 m depth. It is worth noting that these depths correspond to strata characterised by the presence of clayey siltstone to silty claystone, dark greenish grey and slightly bioturbated and containing fragments of diatoms. Hence, it is possible that the third source is related to the settling of biogenic material; such source has not been detected so far in AND-1B sediment core.

Fig. 5 shows the relative contribution of S1, S2 and S3 as a function of the sample depth. S1 and S2 show a very clear opposite pattern: the first gives a major contribution at the lower depths (20–53 m), while S2 is dominant at the higher ones (54–84 m). This pattern, compared with the observations reported by Giorgetti et al. [8], confirms the source attribution. Indeed, as previously reported, these Authors found that the MVG source is dominant during most of the time, while TAM contribution increased up to 50% in the 50–70 m depth interval.
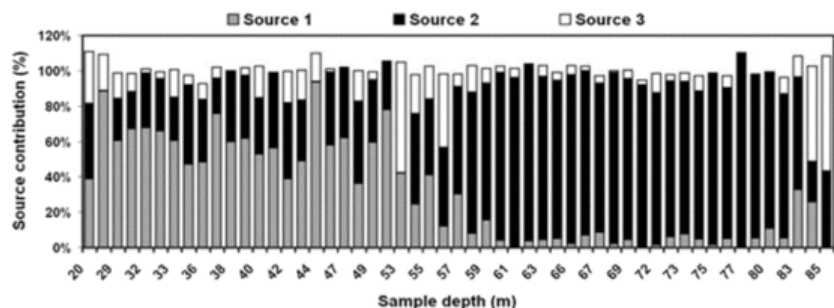

Fig. 5 Source contributions to each sample.

Relative contribution of the three sources identified by PMF analysis (S1, S2 and S3) to each sample as a function of the sample depth.

By joining the main components results here obtained and the conclusions of Giorgetti et al. [8], we attribute S1 to MVG and S2 to TAM sources. Finally, such sources are now better characterised by the REEs and other trace components profiles.

3.2 Climatic implications

An in-depth discussion on the climatic implications of the results here obtained is out of the goal of this paper, but some starting points can be here presented.

Giorgetti et al. [8] report that the TAM source contribution is more evident in the cold periods. Our detailed information on the temporal sequence of the two main sources (S1 = MVG; S2 = TAM) gives us the possibility to verify and improve this statement by comparing the sedimentary history of the first 90 m of the AND-1B core with the EPICA Dome C (EDC) ice core, covering roughly the same temporal interval.

EPICA deep drilling was performed at Dome C (75°06′S, 123°21′E, 3233 m. a.s.l. on the East Antarctic Plateau) down to the depth of 3260 m, during the 2004/05 summer Campaign. It yielded the longest record (8–9 climatic cycles, corresponding to about 900 kyr) ever obtained from an ice core [15]. The paleo-temperature record, reconstructed on the basis of the delta–Deuterium (δD‰) isotopic stratigraphies, allows to identify the temporal sequence of glacial (cold) and interglacial (warm) periods. Referring to Fig. 2 of the paper by Jouzel et al. [15] and using the AND-1B dating, it is possible to roughly assess that the 50–70 m interval in the ANDRILL marine sediment, covering the 860–660 kyr BP period, corresponds to the Marine Isotopic Stages (MIS) from 19 to 16 (note that even numbers identify glacial period, while odd numbers label interglacial periods). Such climatic period is characterised by very low interglacial temperature (negative anomalies) with respect to younger climatic cycles (for instance, MIS 15, 13 and, especially, the most recent MIS 11 and 9). On the same time, the temperature in the MIS 18 and 16 glacial periods reached minimum values (glacial maxima) lower than the younger glacial period (MIS 14). This means that the temperature in the

860–660 kyr BP time interval was lower both in the glacial (cold) and, especially, in the interglacial (warm) periods, with respect to the younger climatic cycles (older cycles were not present in the EDC ice core). This evidence strongly supports that the TMA source contributes in a larger extent to the marine sedimentary materials deposited in the AND-1B drilling site in the coldest periods, when more intense glacial fluxes are supposed to come from the TMA region. On the contrary, in less extreme climatic conditions, the MVG source appears to be dominant, due its short distance from the sediment-core site.

4 Conclusions

We developed an integrated ICP-AES/ICP-SFMS method for the determination of a large number (39) of elements in soils and marine sediments. Analytical performances make the methods suitable for the analysis of the AND-1B sediment core. Major, trace and REEs elements were measured at 1-m resolution in the 24.7–89.0 m depth range, covering roughly the time period 400–1050 kyr.

The PMF statistical analysis allowed a source apportionment on three main sources, characterised by specific source profiles of main and REEs components. The first 2 sources were attributed to terrigenous material coming from the MVG and TMA districts, respectively. A discontinuity was detected in the temporal sequence of the source contributions to the sedimentary material budget. MVG sources were more active in the younger period (660–400 kyr BP), while the TMA source was dominant for the older period. A comparison with the isotopic temperature record of the EDC ice core allowed to assess that TMA glacial fluxes, carrying on terrigenous material, were more intense in the 860–660 kyr BP period, when both glacial and interglacial temperatures were lower that the corresponding younger climatic cycles. This evidence highly support the relevance of interdisciplinary efforts in understanding the feedback processes between climate forcing and environmental responses by a compared study of marine and ice cores.

Acknowledgements

Appendix A. Supplementary data

Supplementary data to this article can be found online at http://dx.doi.org/10.1016/j.microc.2015.04.020.

References

[1]

K.D. Alverson, R.S. Bradley and T.F. Pedersen, Paleoclimate, Global Change and the Future, 2003, Springer Verlag; Berlin Heidelberg, 220.

[2]

M.M. Cheatham, W.F. Sangrey and W.M. White, Sources of error in external calibration ICPMS analysis of geological samples and an improved non-linear drift correction procedure, *Spectrochim. Acta* **48B**, 1993, 487–506.

[3]

J.M. Cook, M.J. Gardner, A.H. Griffiths, M.A. Jessep, J.E. Ravenscroft and R. Yates, The comparability of sample digestion techniques for the determination of metals in sediments, *Mar. Pollut. Bull.* **34** (8), 1997, 637–644.

[4]

S.M. Eggins, J.D. Woodhead, L.P.J. Kinsley, G.E. Mortimer, P. Sylvester, M.T. McCulloch, J.M. Hergt and M.R. Handler, A simple method for the precise determination of ≥ 40 trace elements in geological samples by ICP-MS using enriched isotope internal standardisation, *Chem. Geol.* **134**, 1997, 311–326.

[5]

E.P.I.C.A. Members, Eight glacial cycles from an Antarctic ice core, *Nature* **429**, 2004, 623–628.

[6]

E.P.I.C.A. Members, One-to-one coupling of glacial climate variability in Greenland and Antarctica, *Nature* **444**, 2006, 195–198.

[7]

P. Gabrielli, C. Barbante, C. Turetta, A. Marteel, C. Boutron, G. Cozzi, C. Warren, C. Ferrari and P. Cescon, Direct determination of rare earth elements at the subpicogram per Gram level in Antarctic Ice by ICP-SFMS using a desolvation

system, *Anal. Chem.* **78**, 2006, 1883–1889.

[8]

G. Giorgetti, F. Talarico, S. Sandroni and A. Zeoli, Provenance of Pleistocene sediments in the ANDRILL AND-1B drillcore: clay and heavy mineral data, *Glob. Planet. Chang.* **69**, 2009, 94–102.

[9]

D. Harwood, R. Levy, J. Cowie, F. Florindo, T. Naish, R. Powell and A. Pyne, Deep drilling with the ANDRILL program in Antarctica, *Sci. Drill.* **3**, 2006, 43–45.

[10]

C. Hétmond, C.W. Devey and C. Chauvel, Source compositions and melting processes in the Society and Austral plumes (South Pacific Ocean): element and isotope (Sr, Nd, Pb, Th) geochemistry, *Chem. Geol.* **115**, 1994, 7–45.

[11]

K. Hollocher and J. Ruis, Major and trace element determinations on NIST glass standard reference materials 611, 612, 614 and 1834 by inductively coupled plasma-mass spectrometry, *Geostand. Geoanal.* **19**, 1995, 27–34.

[12]

IPCC, Contribution of Working Groups I, II and III to the Fourth Assessment Report of the Intergovernmental Panel on Climate Change Core Writing Team, In: R.K. Pachauri and A. Reisinger, (Eds.), *IPCC Report 2007,* 2007, 104, (Geneva (Switzerland)).

[13]

J.H.F. Jansen, S.J. Van der Gaast, B. Koster and A.J. Vaars, CORTEX, a shipboard XRF-scanner for element analyses in split sediment cores, *Mar. Geol.* **151**, 1998, 143–153.

[14]

G.A. Jenner, H.P. Longerich, B.J. Fryer and S.E. Jackson, Inductively coupled plasma-mass spectrometric analysis of geological samples: a critical evaluation based on case studies, *Chem. Geol.* **83**, 1990, 105–118.

[15]

J. Jouzel, et al., Orbital and millennial Antarctic climate variability over the past 800,000 years, *Science* **317**, 2007, 793–796.

[16]

M.M. Karadağ, Ş. Küpeli, F. Arýk, A. Ayhan, V. Zedef and A. Döyen, Rare earth element (REE) geochemistry and genetic implications of the Mortaş bauxite deposit (Seydişehir/Konnya – Southern Turkey), *Chem. Erde* **69**, 2009, 143–159.

[17]

P.R. Kyle, Mineral Chemistry of Late Cenozoic McMurdo Volcanic Group Rocks from the Pleiades, Northern Victoria Land, In: E. Stump, (Ed), *Geological Investigations in Northern Victoria Land, Antarctic Research Series* **46**, 1986, AGU; Washington, D.C., 305–333.

[18]

W.E. Le Masurier and J.W. Thomson, (Eds.), *Volcanoes of the Antarctic Plate and Southern Oceans, Antarctic Research Series* **48**, 1990, AGU; Washington, D.C., 97–127.

[19]

Q. Liang and D.C. Gregoire, Determination of trace elements in twenty six Chinese geochemistry reference materials by inductively coupled plasma mass spectrometry, *Geostand. Geoanal.* **24** (1), 2000, 51–63.

[20]

Q. Liang, H. Jing and D.C. Gregoire, Determination of trace elements in granites by inductively coupled plasma mass spectrometry, *Talanta* **51**, 2000, 507–513.

[21]

C.E. McGinnis, J.C. Jain and C.R. Neal, Characterisation of memory effects and development of an effective wash protocol for the measurement of petrogenetically critical trace elements in geological samples by ICP-MS, *Geostand. Newslett.* **21**, 1997, 289–305.

[22]

D. Monien, G. Kuhn, H. von Eynatten and F.M. Talarico, Geochemical provenance analysis of fine-grained sediment revealing Late Miocene to recent Paleo-Environmental changes in the Western Ross Sea, Antarctica, *Glob. Planet. Chang.* **96–97**, 2012, 41–58.

[23]

T. Naish, et al., Obliquity-paced Pliocene West Antarctic ice sheet oscillations, *Nature* **458**, 2009, 322.

[24]

J.A. Olivares and R.S. Houk, Suppression of analyte signal by various concomitant salts in inductively coupled plasma mass spectrometry, *Anal. Chem.* **58**, 1986, 20–25.

[25]

N.J.G. Pearce, J.A. Westgate, W.T. Perkins and S.J. Preece, The application of ICP-MS methods to tephrochronological problems, *Appl. Geochem.* **19**, 2004, 289–322.

[26]

F. Poitrasson, C. Pin, P. Telouk and J.L. Imbert, Assessment of a simple method for the determination of Nb and Ta at the sub μg/g level in silicate rocks by ICPMS, *Geostand. Newslett.* **17**, 1993, 209–215.

[27]

P. Robinson, A.T. Townsend, Z. Yu and C. Münker, Determination of scandium, yttrium and rare earth elements in rocks by high resolution inductively coupled plasma-mass spectrometry, *Geostand. Newslett.* **23** (1), 1999, 31–46.

[28]

G. Schönberg, Simultaneous determination of thirthy-seven trace elements in twenty-eight international rock standards by ICP-MS, *Geostand. Geoanal.* **17**, 1993, 81–97.

[29]

A.L. Sharma, O. Alard, S. Elhlou and N.J. Pearson, Evaluation of perchloric versus nitric acid digestion for precise determination of trace and ultra trace elements by ICP-MS, *J. Conf. Abstr. Goldschmidt* **5** (2), 2000, 914.

[30]

S.D. Tanner, D.J. Douglas and J.B. French, Gas and ion dynamics of a three-aperture vacuum interface for inductively coupled plasma-mass spectrometry, *Appl. Spectrosc.* **48**, 1994, 1373–1378.

[31]

S.R. Taylor and S.M. McLennan, The geochemical evolution of the continental crust, *Rev. Geophys.* **33**, 1995, 241–265.

[32]

Q. Xie, J. Jain, M. Sun, R. Kerrich and J. Fan, ICPMS analysis of basalt BIR-1 for trace elements, *Geostand. Newslett.* **18**, 1994, 53–63.

[33]

T. Yokoyama, A. Makishima and E. Nakamura, Evaluation of the coprecipitation of incompatible trace elements with fluoride during silicate rock dissolution by acid digestion, *Chem. Geol.* **157**, 1999, 175–187.

[34]

Z. Yu, P. Robinson, A.T. Townsend, C. Münker and A.J. Crawford, Determination of high field strength elements, Rb, Sr, Mo, Sb, Cs, Tl, and Bi at ng g^{-1} levels in Geological Reference Materials by magnetic sector ICP-MS after HF/HClO$_4$ high pressure digestion, *Geostand. Geoanal.* **24** (1), 2000, 39–50.

Appendix A. Supplementary data

Multimedia Component 1

Supplementary material.

Highlights

- ICP-AES and ICP-SFMS methods optimized for geochemical analysis of an Antarctic marine sediment core

- 39 main and trace elements and Rare Earth Elements (REEs) determined on the top 90 m of ANDRILL core AND-1B (Antarctica)

- PMF (Positive Matrix Factorization) analysis yielded a source apportionment of the main sources in AND-1b marine core.

- Discontinuity in REEs and metal ratios records was highlighted at 660 kyr BP and likely due to different source dominance.

Queries and Answers

Query:

Please check the presentation and layout of Table 1 if correct.

Answer: It is correct

Query:

Your article is registered as a regular item and is being processed for inclusion in a regular issue of the journal. If this is NOT correct and your article belongs to a Special Issue/Collection please contact c.krishnamoorthy@elsevier.com immediately prior to returning your corrections.

Answer: Yes

Query:

Please confirm that given names and surnames have been identified correctly.

Answer: Yes

Query:

Please check the presentation of data if correct.

Answer: Correct

Query:

The section title "Method setup" is slightly modified fo clarity. Please check.

Answer: Perfectly correct

Query:

Please check the sentence for clarity.

Answer: The sentence sounds as correct to the Authors

Query:

Please check the symbol used here if correct.

Answer: Correct

Query:

This sentence has been slightly modified for clarity. Please check and confirm if the meaning is still correct.

Answer: Correct

Query:

One parenthesis has been deleted to balance the delimiters. Please check and confirm if this was done correctly.

Answer: I confirm, correct

Query:

One parenthesis has been added to balance the delimiters. Please check and confirm if this was done correctly.

Answer: Change correct

Query:

Supplementary caption was not provided. Please check the suggested data if appropriate and correct if necessary.

Answer: No correction needed